Influence of partial dealumination of BEA zeolites on physicochemical and catalytic properties of AgAlSiBEA in H2-promoted SCR of NO with ethanol

Nataliia O. Popovych, Pavlo I. Kyriienko, Sergiy O. Soloviev, Svitlana M. Orlyk, Stanislaw Dzwigaj

▶ **To cite this version:**

Nataliia O. Popovych, Pavlo I. Kyriienko, Sergiy O. Soloviev, Svitlana M. Orlyk, Stanislaw Dzwigaj. Influence of partial dealumination of BEA zeolites on physicochemical and catalytic properties of AgAlSiBEA in H2-promoted SCR of NO with ethanol. Microporous and Mesoporous Materials, 2016, 226, pp.10-18. 10.1016/j.micromeso.2015.12.031 . hal-01259919

HAL Id: hal-01259919

https://hal.sorbonne-universite.fr/hal-01259919

Submitted on 21 Jan 2016

HAL is a multi-disciplinary open access archive for the deposit and dissemination of scientific research documents, whether they are published or not. The documents may come from teaching and research institutions in France or abroad, or from public or private research centers.

L'archive ouverte pluridisciplinaire **HAL**, est destinée au dépôt et à la diffusion de documents scientifiques de niveau recherche, publiés ou non, émanant des établissements d'enseignement et de recherche français ou étrangers, des laboratoires publics ou privés.

ACCEPTED MANUSCRIPT

Influence of partial dealumination of BEA zeolites on physicochemical and catalytic properties of AgAlSiBEA in H_2-promoted SCR of NO with ethanol

Nataliia O. Popovych,*[a] Pavlo I. Kyriienko,[a] Sergiy O. Soloviev,[a] Svitlana M. Orlyk[a] and Stanislaw Dzwigaj*[b,c]

[a] L.V. Pisarzhevskii Institute of Physical Chemistry of the National Academy of Sciences of Ukraine, 31 Prosp. Nauky, 03028 Kyiv, Ukraine Fax: +38 044 525 65 90.

[b] Sorbonne Universités, UPMC Univ Paris 06, UMR 7197, Laboratoire de Réactivité de Surface, F-75005 Paris, France. E-mail: stanislaw.dzwigaj@upmc.fr

[c] CNRS, UMR 7197, Laboratoire de Réactivité de Surface, F-75005, Paris, France

Figures: 10

Keywords: hydrogen, SCR, NO, silver, BEA zeolite

* Corresponding authors:

N. Popovych, E-mail address: natalie.popovych@ukr.net, fax: +38 (044) 525 65 90.

S. Dzwigaj, E-mail address: stanislaw.dzwigaj@upmc.fr, fax: +33 01 44 27 60 33.

ACCEPTED MANUSCRIPT

ACCEPTED MANUSCRIPT

Abstract

The two-step postsynthesis method allows obtaining AlSiBEA zeolites with different degree of dealumination (Si/Al=100 and 200). Physicochemical properties (crystallinity, hydroxyl group coverage, acidic sites and nature of silver species) of AlSiBEA and AgAlSiBEA were investigated by XRD, DR UV-vis, XPS, TEM and FT-IR with CO and pyridine as probe molecules. Catalytic properties of the zeolites were studied in the process of selective reduction of NO with ethanol in the presence of hydrogen in the reaction mixture. It was shown that level of H_2-promoting effect on the SCR-process depends on the dealumination degree of Ag-containing BEA zeolites and greater effect is observed for the catalysts with higher concentration of Lewis acidic sites.

ACCEPTED MANUSCRIPT

1. Introduction

Nitrogen oxides (NO_x) abatement in exhaust gases of lean-burn and diesel engines remains a target for environmental catalysis research. Metal-containing zeolites are known to be promising catalysts for selective catalytic reduction (SCR) of NO_x with hydrocarbons and oxygenates [1]. Activity of zeolite catalysts depends on the nature of added metal (Cu, Fe, Co, Ag) as well as on the framework type (MFI, BEA, MOR, FAU) [2-4]. Interest in silver-containing catalysts was stimulated after the finding that addition of hydrogen into the reaction mixture enhances the selective reduction of NO_x [5]. The origin of this effect is still under debate, *i.e.*, the role of H_2 in the reaction mechanism and structural changes of silver active sites [6-15]. It is most likely that in order to increase the rate of NO_x conversion hydrogen must accelerate a rate-determining step of the reaction [6,7]. The enhanced activity after H_2 addition was assigned to the formation of the nitrite species that are more reactive than adsorbed nitrate species in C_3H_6-SCR reaction on Ag/Al_2O_3 [7,8]. Other way of hydrogen effect was suggested to be the formation of active oxygen species on Ag clusters on Ag/Al_2O_3 and Ag-MFI catalysts [9,10], which promote partial oxidation of hydrocarbons to surface acetate [11] or enolic species [12]. Formation of the key intermediate of isocyanate from cyanide was also considered as the rate-determining step and was suggested to be promoted by hydrogen [6,13-15].

However, silver ions and clusters were considered only as active sites of the hydrogen-promoted SCR of NO_x with hydrocarbons or oxygenates and influence of the acidic sites has not been taken into consideration. It was only proposed [16] that variation in catalytic activity of Ag-containing zeolites in C_3H_8-SCR of NO in the presence of H_2 arises from the support effect on the ratio of Ag species, which was shifted to cationic side with the increase of amount and strength of acidic sites in zeolites. The effect of acidic properties of Ag/Al_2O_3 catalysts on their activity in the SCR of NO_x with hydrocarbons or oxygenates was highlighted in several recent studies [17-19].

ACCEPTED MANUSCRIPT

In a previous work [20], we have shown that promoting H_2-effect in the SCR of NO with ethanol is observed in the presence of AgBEA (with Si/Al ratio equal to 12.5), whereas it is almost absent on Ag-containing catalysts based on dealuminated BEA (Si/Al=1000). It was concluded that a necessary condition for H_2-effect is the presence of silver clusters in close proximity to strong Lewis acidic sites (LAS) in the zeolite catalysts. Therefore, it is expedient to study the influence of intermediate degree of dealumination (12.5 < Si/Al < 1000) on the appearance of H_2-effect.

For this purpose Ag-containing partially dealuminated BEA zeolites (with Si/Al ratio of 100 and 200) were prepared using the two-step postsynthesis method [21-24]. The present work aimed to investigate the influence of partial dealumination of AgBEA zeolites on their physicochemical properties (crystallinity, acidity, nature of silver species) and catalytic performance in the H_2-promoted SCR of NO with ethanol.

2. Experimental

2.1. Catalysts preparation

Silver containing BEA zeolite was prepared by the two-step postsynthesis method: in the first step, TEABEA zeolite provided by RIPP (China) was treated in 6 or 8 $mol \cdot L^{-1}$ HNO_3 aqueous solution (353 K) to obtain partially dealuminated supports AlSiBEA (Si/Al = 100) or AlSiBEA (Si/Al = 200) with the vacant T-atom sites (T = Al). Then the suspension was recovered by centrifugation, washed with distilled water and dried at 353 K. The resulting partially dealuminated zeolites were labeled as AlSiBEA(100) and AlSiBEA(200), where Si/Al ratio was marked in parenthesis.

To prepare Ag-containing zeolites, 2 g of AlSiBEA (Si/Al = 100) and AlSiBEA (Si/Al = 200) was firstly stirred under aerobic conditions for 2 h at 298 K in 200 mL of $AgNO_3$ (Fluka silver nitrate with high Ph Eur purity with Ag >99.8%) aqueous solution (pH = 2.3) with different concentrations of 0.9, 2.7 and $5.4 \cdot 10^{-3}$ $mol \cdot L^{-1}$ to obtain the zeolites with various Ag

ACCEPTED MANUSCRIPT

content. Then the suspension was stirred in evaporator under vacuum of a water pump for 2 h in air at 353 K until the water was evaporated. The resulting solid containing 0.5, 1.5 and 3.0 Ag wt % were labeled as $Ag_{0.5}$AlSiBEA(100), $Ag_{1.5}$AlSiBEA(100) and $Ag_{3.0}$AlSiBEA(100) or $Ag_{0.5}$AlSiBEA(200), $Ag_{1.5}$AlSiBEA(200) and $Ag_{3.0}$AlSiBEA(200), respectively, with Si/Al ratio marked in parenthesis.

Preparation and physicochemical properties of AgAlBEA and AgSiBEA were described earlier [25,26]. To prepare AgAlBEA zeolite, firstly, the TEABEA zeolite was calcined at 823 K for 15 h to obtain AlBEA (Si/Al=12.5) and secondly, the latter was impregnated with $AgNO_3$ aqueous solution. AgSiBEA zeolite was prepared by the two-step postsynthesis method: treatment of TEABEA zeolite in 13 mol·L^{-1} HNO_3 aqueous solution (4 h, 353 K) in the first step to obtain a dealuminated (Si/Al=1000) and organic-free SiBEA support and stirring of SiBEA under aerobic conditions for 2 h at 298 K in 200 ml of aqueous $AgNO_3$ solution followed by stirring in evaporator under vacuum of the water pump for 2 h in air at 353 K until evaporation of the water.

2.2 Catalysts characterization

X-Ray Fluorescence chemical analysis was performed at room temperature on a SPECTRO X-LabPro apparatus.

Powder X-ray diffraction (XRD) was recorded at room temperature and ambient atmosphere on a Bruker D8 Advance diffractometer using the CuKα radiation (λ = 154.05 pm).

Analysis of the acidic properties of samples was performed by adsorption of pyridine and CO followed by Fourier transform infrared spectroscopy (FT-IR). Before analysis, the samples were pressed at ≈1 ton·cm^{-2} into thin wafers of ca. 10 mg·cm^{-2} and placed inside the IR cell.

Before CO adsorption experiment, the wafers were activated by calcination at 723 K for 2 h in flowing 2.5 % O_2/Ar and then outgassed at 573 K (10^{-3} Pa) for 1 h. Following thermal treatment, the samples were cooled down to 100 K. CO was introduced in increasing amounts up to an equilibrium pressure of 133 Pa. Infrared spectra were recorded using a Bruker Vertex 70

ACCEPTED MANUSCRIPT

spectrometer (resolution – 2 cm^{-1}, 128 scans). The spectra were obtained after subtraction of the spectrum recorded after calcination and prior to CO adsorption.

Before pyridine adsorption/desorption experiments, the wafers were activated by calcination in static conditions at 773 K for 1 h in O_2 ($2 \cdot 10^4$ Pa) (or in H_2 flow) and then outgassed under secondary vacuum at 673 K (10^{-3} Pa) for 1 h. The wafers were contacted at 423 K with gaseous pyridine. The spectra were recorded after pyridine desorption at 423, 573 and 673 K using Spectrum One FT-IR spectrometer (resolution – 1 cm^{-1}, 12 scans). The reported spectra were obtained after subtraction of the spectrum recorded after calcination and prior to pyridine adsorption.

Diffuse reflectance (DR) UV-vis spectra were recorded at ambient atmosphere on a Cary 5000 Varian spectrometer equipped with a double integrator with polytetrafluoroethylene as reference.

2.3 Catalytic tests

Catalytic activity tests were carried out in a fixed-bed flow quartz reactor at atmospheric pressure. Samples with grains of 0.5-1.0 mm (0.5 cm^3, ≈0.3 g) were loaded into the reactor. Gas feed for the reaction was 500 ppm NO, 1000 ppm C_2H_5OH, 10 % O_2, 0.5% H_2 in He with the gas hour space velocity of 24,000 h^{-1}. The gas feed was adjusted by mass-flow controllers (Chromatek-Crystal FGP). Before reaction, the catalyst was heated to 773 K at a heating rate of 20 degrees$\cdot min^{-1}$ in a flow of O_2/He (or H_2/He when hydrogen was added to the reaction mixture) and held for 1 h, then cooled to 453 K with a further step-heating in reaction gas feed to a temperature of conversion measurement. The steady-state activity was measured after 30 min reaction at a certain temperature. The temperature was controlled through an Autonics TZN4S temperature controller using a chromel-alumel thermocouple. The concentration of NO was continuously monitored using a chemiluminescence gas analyzer (344HL04, Ukraine). The products were analyzed by gas chromatograph (TCD) (Kristallyuks 4000M, Metachrom, Russia) with a CaA column (for NO, N_2, CO) and a Polisorb-1 column (for N_2O, CO_2, C_2H_4, ethanol).

ACCEPTED MANUSCRIPT

Catalytic activity was characterized by NO conversion to N_2 and temperatures of its achievement.

3. Results and Discussion

3.1. Characterization of AlSiBEA and AgAlSiBEA

3.1.1. Crystallinity of the samples

X-ray diffractograms of AlSiBEA(100) and AlSiBEA(200), i.e., after partial removal of aluminium atoms, are similar with TEABEA zeolite calcined at 823 K for 15 h (AlBEA(12.5)) [25,26], suggesting that the dealumination does not significantly affect the structure and crystallinity of BEA zeolite are preserved (Fig. 1).

A narrow diffraction peak near 22.5° is generally taken as evidence of lattice contraction/expansion of the BEA structure [27,28]. The d_{302} spacing, calculated from the corresponding 2θ value, decreases from 3.950 Å (AlBEA with 2θ of 22.48°) [26] to 3.947 Å (AlSiBEA(100) with 2θ of 22.50°) and to 3.940 Å (AlSiBEA(200) with 2θ of 22.54°) suggesting a matrix contraction, consistent with the removal of aluminium from the zeolite framework.

Upon introduction of 1.5 and 3.0 Ag wt % into AlSiBEA(100) the d_{302} spacing increases from 3.947 Å to 3.950 Å ($Ag_{1.5}$AlSiBEA(100) with 2θ of 22.48°) and to 3.956 Å ($Ag_{3.0}$AlSiBEA(100) with 2θ of 22.45°) (Fig. 1A). For the sample with the Si/Al ratio equal to 200 (Fig. 1B), d_{302} spacing increases after silver introduction from 3.940 Å to 3.945 Å ($Ag_{1.5}$AlSiBEA(200) with 2θ of 22.51°) and to 3.947 Å ($Ag_{3.0}$AlSiBEA(200) with 2θ of 22.50°). This increase can be taken as an evidence of framework expansion of the BEA structure and suggests incorporation of silver ions ~~into the vacant T-atom sites of~~ in the framework of AlSiBEA zeolite, in line with earlier reports [21,29].

3.1.2. FT-IR characterization of the hydroxyl groups

AlSiBEA(100), $Ag_{1.5}$AlSiBEA(100), AlSiBEA(200) and $Ag_{1.5}$AlSiBEA(200) zeolites have been investigated by FT-IR spectroscopy in the range of vibration of OH groups (Fig. 2).

ACCEPTED MANUSCRIPT

As was shown earlier [25,26], the FT-IR spectrum of AlBEA(12.5) exhibits four main IR bands due to the OH stretching modes of Al-OH (bands at 3781 and 3667 cm^{-1}), zeolite acidic hydroxyls Al-O(H)-Si (band at 3615 cm^{-1}) and Si-OH groups (band at 3750 cm^{-1} with a shoulder at 3740 cm^{-1}). The treatment of TEABEA zeolite by aqueous acid nitric solution leads to the partial dealumination of the framework as evidenced by the absence of bands at 3781 and 3667 cm^{-1} and presence of the band at 3615-3630 cm^{-1} on the spectra of AlSiBEA(100) and AlSiBEA(200) (Fig. 2). Bands at 3709-3714 cm^{-1} related to terminal internal silanol groups and broad bands at 3490-3520 cm^{-1} due to H-bonded Si-OH groups evidence creation of vacant T-atom sites associated with silanol groups upon partial removal of framework aluminium, in line with earlier assignments [21,29].

Upon introduction of 1.5 Ag wt % in AlSiBEA(100) and AlSiBEA(200) intensity of the bands at 3615-3630 cm^{-1} and 3490, 3529 cm^{-1} decreased indicating that some of the Al-O(H)-Si and hydrogen bonded Si-OH groups have been consumed during their reaction with silver precursor.

3.1.3. Characterization of acidic sites: FT-IR spectroscopy with CO and pyridine

To determine the nature, number and strength of acidic sites in the partially dealuminated BEA samples FT-IR spectra of adsorbed CO (Figs. 3-4) and pyridine (Fig. 5) as probe molecules were taken.

Difference spectra between FT-IR spectra in OH stretching region recorded after and before CO adsorption on AlSiBEA(100), $Ag_{1.5}$AlSiBEA(100), AlSiBEA(200) and $Ag_{1.5}$AlSiBEA(200) at 100 K are given in Fig. 3. The adsorption of CO at 100 K (100 Pa equilibrium pressure) leads to appearance of intense positive bands at 3645, 3595, 3445, 3290 cm^{-1} and negative bands at 3739, 3715 and 3615 cm^{-1}. The intensity of the bands at 3645 and 3595 cm^{-1} quickly decreases during outgassing of CO, while the bands at 3739 and 3715 cm^{-1} are restored. The observed shift of 94 cm^{-1} from 3739 to 3645 cm^{-1} for isolated external Si-OH groups and 120 cm^{-1} from 3715 to 3595 cm^{-1} for terminal internal Si-OH groups indicate that

ACCEPTED MANUSCRIPT

these silanol groups in all samples have weak acidic character. The low intensity of positive bands at 3445 and 3290 cm^{-1} related to red shifted bands of perturbed Al-O(H)-Si groups [30-32], suggests that only a little amount of these acidic hydroxyls groups occur in the partially dealuminated zeolites.

For $Ag_{1.5}$AlSiBEA(100) and $Ag_{1.5}$AlSiBEA(200) lower intensity of the bands at 3645, 3595, 3445 and 3290 (absence for $Ag_{1.5}$AlSiBEA(200)) cm^{-1} indicates reaction of Al-O(H)-Si and hydrogen bonded Si-OH groups with silver precursor.

Figure 4 shows the changes in the carbonyl region when CO is adsorbed on AlSiBEA(100), $Ag_{1.5}$AlSiBEA(100), AlSiBEA(200) and $Ag_{1.5}$AlSiBEA(200). In the case of AlSiBEA(100) and AlSiBEA(200) under CO equilibrium pressure of 100 Pa, carbonyl bands are detected at 2175, 2157, 2140 and 2134-2135 cm^{-1} (Fig. 4, spectrum a). The bands at 2140 and 2134-2135 cm^{-1} are assigned to weakly bonded physically adsorbed CO [33,34] and disappear first upon outgassing. The next band to disappear is that at 2157 cm^{-1}. It changes simultaneously with the band at 3645 cm^{-1} allowing assigning 2157 cm^{-1} band to CO bonded to silanol groups present in vacant T-atom sites [24]. Further sample outgassing provokes disappearance of the band at 2175 cm^{-1} (Fig. 4, spectra b-f), typical of CO interacting with bridging Al-O(H)-Si hydroxyls. Low intensity bands at 2185 and 2225 cm^{-1} (spectra f) correspond to Al^{3+}-CO vibrations with Al in framework and extraframework positions remained in the zeolite structures after dealumination.

For $Ag_{1.5}$AlSiBEA(100) and $Ag_{1.5}$AlSiBEA(200) four main bands at 2184, 2157, 2140 and 2135-2137 cm^{-1} appear. The positions of three bands at 2157, 2140, 2135-2137 cm^{-1} are the same as those observed for AlSiBEA(100) and AlSiBEA(200) and can be assigned to CO interacting with silanol groups (band at 2157 cm^{-1}) and to physically bonded CO (bands at 2140 and 2135-2137 cm^{-1}). In contrast, the intensity of the band at 2157 cm^{-1} for $Ag_{1.5}$AlSiBEA(100) and $Ag_{1.5}$AlSiBEA(200) is much lower than that observed for silver-free zeolites. It proves the consumption of silanol groups as a result of reaction with silver ions. ~~upon incorporation of~~

ACCEPTED MANUSCRIPT

~~silver ions in the vacant T-atom sites of the zeolites.~~ The decreasing of the intensities of the bands of silanol groups after ~~incorporation of~~ reaction with silver ions ~~in the vacant T-atom sites~~ is accompanied by the appearance of the band at 2184 cm^{-1} which could be assigned to ν(CO) stretching vibration of Ag^{+}-CO complexes.

Difference spectra between FT-IR spectra recorded after and before pyridine adsorption on AlSiBEA(100), $Ag_{3.0}$AlSiBEA(100), AlSiBEA(200) and $Ag_{3.0}$AlSiBEA(200) are shown in Fig. 5. For AlSiBEA(100) and AlSiBEA(200), the bands typical of pyridinium cations are observed at 1638 and 1547 cm^{-1}, indicating the presence of Brønsted acidic sites. These sites are related to the acidic proton of Al-O(H)-Si groups, in line with earlier data obtained for BEA zeolite [24,29].

The bands at 1622 and 1455 cm^{-1} are related to pyridine interacting with strong Lewis acidic sites (Al^{3+}) while the one at 1600 cm^{-1} corresponds to pyridine interacting with weak Lewis acidic sites, the band 1448 cm^{-1} could be related to pyridine interacting with weak Lewis acidic sites and/or physisorbed pyridine. The band at 1491 cm^{-1} corresponds to pyridine interacting with both Brønsted and Lewis acidic sites.

Desorption at increasing temperatures resulted in the appearance of a new band at 1463 cm^{-1} (Fig. 5, spectra c), which was assigned to iminium ions formed by the attack of protons on the pyridine complex bonded to Lewis acidic sites [35]. However, there is also other possible explanation for the presence of the bands at 1455 and 1463 cm^{-1} – the band of higher frequency represents Lewis sites of a higher relative acid strength [36]. The adsorption bands of pyridinium cations and pyridine bonded to LAS are present in the FT-IR spectra even after outgassing at 673 K (Fig. 5, spectra c), suggesting the presence of strong Brønsted and Lewis acidic sites. The difference between FT-IR spectra of pyridine adsorbed on AlSiBEA(100) and AlSiBEA(200) is lower intensity of the bands for AlSiBEA(200) spectra, indicating the lower concentration of Brønsted and Lewis acidic sites, which are related to number of Al atoms remaining in BEA zeolite after dealumination.

ACCEPTED MANUSCRIPT

The incorporation of silver in AlSiBEA(100) and AlSiBEA(200) leads to appearance of new bands with high intensity at 1605 and 1450 cm^{-1}, as shown for $Ag_{3.0}$AlSiBEA(100) and $Ag_{3.0}$AlSiBEA(200) in Fig. 5, suggesting the formation of silver Lewis acidic sites. Formation of new LAS after the introduction of silver was also observed for AlBEA(12.5) and SiBEA(1000) zeolites [25,26]. Lower intensity of the bands at 1638, 1547 and 1491 cm^{-1} indicates decrease in concentration of Brønsted acidic sites due to consumption of some Al-O(H)-Si and hydrogen bonded Si-OH groups during their reaction with silver precursor. Increase in concentration of Lewis acidic sites after introduction of silver (3.0 wt %) in AlSiBEA(100) is greater than that observed in AlSiBEA(200) (Fig. S1 in Supplementary material). It is likely that higher amount of Lewis acidic sites are formed when they include unsaturated aluminum and silver species.

Fig. 6 shows FT-IR spectra of adsorbed pyridine on AlSiBEA(100), $Ag_{3.0}$AlSiBEA(100) and $Ag_{3.0}$AlSiBEA(200) zeolites reduced in H_2 flow. As could be seen for AlSiBEA(100) reduction in hydrogen almost does not change the bands corresponding to Brønsted and Lewis acidic sites (Fig. 5A, a and Fig. 6). For reduced $Ag_{3.0}$AlSiBEA(100) and $Ag_{3.0}$AlSiBEA(200) decrease in intensity of the bands at 1450 and 1605 cm^{-1} is observed as well as increase of band at 1491 cm^{-1}. It is probable that not all Ag species are reduced with H_2 and some amount of silver-containing LAS is remained.

3.1.4. Nature of silver species

Silver state in the zeolites was investigated by DR UV-vis, X-ray photoelectron spectroscopy (XPS), and transmission electron microscopy (TEM).

Fig. 7 shows the DR UV-vis spectra of $Ag_{3.0}$AlSiBEA(100) and $Ag_{3.0}$AlSiBEA(200) zeolites after pre-treatment in the conditions of H_2-promoted SCR of NO with ethanol. For both samples there are four main bands at 225, 260, 286 and 412 nm. The absorbance in the region below 250 nm is generally attributed to electronic transitions from $4d^{10}$ to $4d^{9}5s^{1}$ of highly dispersed Ag^{+} ions [37-39]. The bands observed at 260 and 286 nm are assigned to $Ag_n^{\delta+}$ clusters

ACCEPTED MANUSCRIPT

($2 \leq n \leq 4$) [40]. The absorption at wavelengths >390 nm is attributed to nanoparticles of metallic silver (Ag_m^0) [38]. Intensity of the band at 225 nm is higher for $Ag_{3.0}$AlSiBEA(100) zeolite, whereas bands at 260 and 286 nm are more intensive on $Ag_{3.0}$AlSiBEA(200) spectrum, which may indicate that $Ag_{3.0}$AlSiBEA(100) contains more Ag^+ ions and less $Ag_n^{\delta+}$ clusters than $Ag_{3.0}$AlSiBEA(200). It is likely that some silver ions remain incorporated in the framework of partially dealuminated zeolite even after the SCR-process. Higher amount of Ag^+ ions in $Ag_{3.0}$AlSiBEA(100) explains greater increase of Lewis acidity upon introduction of silver in AlSiBEA(100) than AlSiBEA(200) (Fig. S1 in Supplementary material), since silver ions act as Lewis acids.

The presence of well dispersed oxidized silver species in AgAlSiBEA(100) and AgAlSiBEA(200) is confirmed by XPS (Fig. S2 in Supplementary material). Peak at binding energy of 368.4-368.5 eV (Ag $3d_{5/2}$) and 374.4-374.5 eV (Ag $3d_{3/2}$) are close to values reported earlier for silver well dispersed in zeolites [41,42].

Nanoparticles of silver with the average size of 8-9 nm were detected on TEM images of $Ag_{3.0}$AlSiBEA(100) and $Ag_{3.0}$AlSiBEA(200) zeolites after pre-treatment in the conditions of H_2-promoted SCR of NO with ethanol (Fig. S3 in Supplementary material). The interplanar spacing equal to 3.958 Å for $Ag_{3.0}$AlSiBEA(100) and 3.943 Å for $Ag_{3.0}$AlSiBEA(200) can be attributed to the d_{302} spacing of BEA zeolite, which corroborate the XRD results. For $Ag_{3.0}$AlSiBEA(100), d_{hkl} spacing, equal to 1.141, 2.051 and 2.802 Å, can be attributed to (222), (200) planes of the face-centred cubic metallic silver and (111) plane of Ag_2O, respectively. Diffraction rings on pattern of $Ag_{3.0}$AlSiBEA(200) (with d_{hkl} of 0.800 and 1.154 Å) can be assigned to (331) and (222) planes of the face-centred cubic metallic silver and (211) plane of Ag_2O (d_{hkl}=1.934 Å).

3.2 Catalytic properties of AgAlSiBEA zeolites

Figures 8 A, B show the temperature dependences of NO conversion in the SCR with ethanol on AgAlSiBEA(100) and AgAlSiBEA(200) zeolite catalysts. It should be noted that N_2O, the undesirable by-product of the SCR of NO reaction (due to its large greenhouse gas

ACCEPTED MANUSCRIPT

potential) was not formed in the conditions of the catalytic experiments. The SCR-activity of AlSiBEA(100) and AlSiBEA(200) supports is low, *i.e.*, NO conversion does not exceed 10 % in all temperature range of the reaction (curves 1, 5). The maximally achieved NO-to-N_2 conversion at 725 K after the introduction of 0.5, 1.5 and 3.0 wt % of Ag in AlSiBEA(100) is equal to 12, 24 and 36 %, respectively (Fig. 8A, curves 2-4).

For AlSiBEA(200)-based samples, NO conversion increases to 24 and 26 % at 625 K after the incorporation of 1.5 and 3.0 wt % of silver and almost the same for $Ag_{0.5}$AlSiBEA(200) and AlSiBEA(200) catalysts (Fig. 8B). Conversion of ethanol to CO_2, CO and ethylene in the SCR-process is shown in Fig. 9. When silver loading is increased from 0.5 to 3.0 wt % in both AgAlSiBEA(100) and AgAlSiBEA(200) catalysts, ethanol conversion to CO_2 is enhanced (curve 1) and to CO and ethylene is notably decreased (curves 2, 3). Obviously, at higher Ag content ethanol activation by oxidation on silver species predominates over dehydration on acidic sites, which leads to higher NO-to-N_2 conversion (Fig. 8). The main C-containing product during the SCR of NO on $Ag_{3.0}$AlSiBEA(100) and $Ag_{3.0}$AlSiBEA(200) is CO_2, however for the catalyst with higher concentration of acidic sites (Si/Al=100) ethylene is observed in the reaction products up to 675 K. Decrease in ethanol conversion to ethylene with temperature rising for all catalysts may be caused by less rate of C_2H_5OH dehydration with C_2H_4 formation and/or by ethylene participation in the SCR of NO. Thus, on $Ag_{1.5}$AlSiBEA(200) (Fig. 9, curve 3) sharp decrease in ethanol conversion to C_2H_4 is observed at 625 K, when the maximal NO conversion is achieved (Fig. 8, curve 7).

Almost the same NO conversion is achieved for samples with different degree of dealumination and equal Ag content at temperatures up to 625 K (Fig. 8). However at higher temperatures (> 625 K) NO conversion on AgAlSiBEA(100) still increases and on AgAlSiBEA(200) decreases. Apparently, in the presence of sample with lower Brønsted and Lewis acidity the rate of reductant oxidation by O_2 is increased with temperature rising and participation of ethanol in reduction of NO is decreased.

ACCEPTED MANUSCRIPT

Role of silver species (Ag^+ cations and $Ag_n^{\delta+}$ clusters) consists in the activation of alcohols, adsorbed on silver LAS, by their partial oxidation with formation of more reactive intermediates (enolic species) [18,20,43]. Activation of NO_x occurs on Lewis acidic sites [44]. In the presence of AgAlSiBEA(100), containing higher amount of acidic sites on which enolic and nitrate intermediates are adsorbed, with temperature rising the rate of NO SCR is increased.

The increasing of NO conversion in the SCR with ethanol after hydrogen addition is observed from 10% to 26% on $Ag_{0.5}$AlSiBEA(100), from 24% to 50% in the presence of $Ag_{1.5}$AlSiBEA(100) and for $Ag_{3.0}$AlSiBEA(100) – from 34% to 56% at 675 K (Fig. 8A). The effect of hydrogen is less significant for AlSiBEA(200)-based samples, namely, NO conversion increased from 6% to 17% on $Ag_{0.5}$AlSiBEA(200), from 23% to 28% on $Ag_{1.5}$AlSiBEA(200) and from 25% to 40% on $Ag_{3.0}$AlSiBEA(200) (Fig. 8B). H_2 effect on the SCR-process on AgAlSiBEA catalysts is reversible – after removal of hydrogen from the gas feed, conversion of NO is decreased to the value achieved before H_2 addition. Moreover, hydrogen is not a selective reductant of NO (reduction does not occur in the absence of ethanol in the reaction mixture).

Therefore, it seems that level of H_2-promoting effect depends on both silver loading and zeolite component of the catalyst; and higher effect is observed for the catalysts with lower Si/Al ratio. This assumption is supported by our previous investigations [20], *i.e.*, promoting H_2-effect on the SCR of NO with ethanol was observed in the presence of AgAlBEA(12.5) catalysts, whereas was almost absent on AgSiBEA(1000). Fig. 10 shows increase in NO conversion after hydrogen addition in the presence of the silver-containing BEA zeolites with different Si/Al ratio. This Figure reveal an extreme dependence of H_2-effect on silica/alumina ratio, *i.e.*, the promoting effect is enhanced when Si/Al increase from 12.5 to 100 and then diminish with further increase of this ratio. This tendency may be caused by the similar change of the concentration of Lewis acidic sites, which are present in studied BEA supports as a result of silver introduction in the zeolites.

ACCEPTED MANUSCRIPT

The addition of hydrogen in the reaction mixture changes the distribution of ethanol conversion products in the SCR of NO (Fig. 9, curves marked with asterisks). For all catalysts, CO_2 content is increased and amount of products of partial oxidation (CO) and dehydration (ethylene) is decreased in H_2 presence. The most noticeable changes are observed on $Ag_{1.5}$AlSiBEA(100): ethanol conversion to CO_2 is increased from 15 to 56% with simultaneous decreasing to C_2H_4 in the temperature range of the reaction. It should be underlined that in the presence of $Ag_{1.5}$AlSiBEA(100) the highest enhancement of NO conversion is observed after H_2 addition (Fig. 8A, curves 3,3*). Thus, in the conditions of our experiments hydrogen addition increases the rate of ethanol oxidation, while simultaneously inhibits the process of ethanol dehydration. The similar effect of promotion of ethanol partial oxidation and suppression of ethanol dehydration and dehydrogenation was observed for the SCR process after hydrogen addition on Ag/Al_2O_3 [45].

Promotion of SCR process with H_2 may be caused by the formation of peroxide-like species on silver clusters after dissociation of hydrogen with subsequent formation of H-Ag_4^{2+}-H, where activation of O_2 occurs, followed by formation of hydrogen peroxide species (HOO-Ag_4^{2+}-H) [11]. During the reaction of reductant molecules with HOO^- partially oxidized intermediates are formed. The suggestion that role of hydrogen in the mechanistic pathways of the SCR process consists in the generation of highly reactive hydroxyl and hydroperoxy species is supported by the fact of increasing NO conversion in the SCR with decane after addition of hydrogen peroxide [46].

Furthermore, in the presence of H_2 in the reaction mixture the stability of surface nitrate species is strongly decreased and they are readily transformed on silver sites to the reactive nitrite complexes [8,47-50]. However if only the activation of reagents with formation of more reactive intermediates (enolic and/or nitrite) on silver clusters was a reason of hydrogen promoting effect, the same increase in NO conversion would be observed on both AgAlSiBEA(100) and AgAlSiBEA(200).

ACCEPTED MANUSCRIPT

We can assume that the presence of Lewis acidic sites on the catalyst surface is necessary to H_2-effect occurrence in the SCR of NO. It was shown recently[51] that for H_2 activation on θ-Al_2O_3(110)-supported Ag clusters the interfacial cooperative mechanism between the Ag cluster and Lewis acid-base pair site (Al-O site) is relevant, because H_2 dissociation at the silver-alumina interface is thermodynamically preferred compared with silver clusters. The reason of greater promoting effect on partially dealuminated AgAlSiBEA(100) with higher LAS content than AgAlSiBEA(200) may be connected with enhanced H_2 activation. Alternatively, the higher surface concentration of nitrite-nitrate species adsorbed on Lewis acidic sites of AgAlSiBEA(100) is sufficient to react with products of ethanol activation. For the AgAlSiBEA(200) catalysts with lower LAS concentration higher rate of reagents activation in the presence of hydrogen may be annihilated by their deficient surface concentration.

Thus, the design of active Ag-containing catalysts for the H_2-promoted SCR process should include creation of two types of active sites – silver nanoclusters and Lewis acidic sites with the optimal concentration on the surface.

Conclusions

The two-step postsynthesis method used in this work allows obtaining BEA zeolites with different degree of dealumination (with Si/Al ratio of 100 and 200) without lost of their crystallinity and incorporating Ag ions into ~~the vacant T-atom sites of the~~ zeolite framework.

Introduction of silver in partially dealuminated zeolite leads to the formation of new Lewis acidic sites as shown by FT-IR spectroscopy with adsorption of pyridine and CO. Increase in concentration of Lewis acidic sites after silver addition (3.0 wt %) in AlSiBEA (Si/Al=100) is greater than in AlSiBEA (Si/Al=200).

The presence of well dispersed silver species (silver ions incorporated in the framework of the zeolites, small $Ag_n^{\delta+}$ clusters ($2 \leq n \leq 4$) and nanoparticles with the average size of 8-9 nm) in AgAlSiBEA samples is evidenced by combined use of diffuse reflectance UV-vis, XPS and TEM.

ACCEPTED MANUSCRIPT

The temperature range of increasing conversion of NO in the SCR process with ethanol on AgAlSiBEA(100) catalysts is wider compared to AgAlSiBEA(200). This may be caused by the excess of rate of deep reductant oxidation by O_2 over selective NO reduction with temperature rising above 625 K in the presence of sample with lower Brønsted and Lewis acidity.

Level of H_2-promoting effect on the process of SCR of NO with ethanol depends on the dealumination degree of Ag-containing BEA zeolite catalysts and greater effect is observed for the catalysts with higher concentration of surface acidic sites.

References

[1] B. Moden, J.M. Donohue, W.E. Cormier, H.-X. Li, Top. Catal. 53 (2010) 1367.

[2] J. Janas, S. Dzwigaj, Catal. Today 176 (2011) 272.

[3] L. Li, N. Guan, Microporous Mesoporous Mater. 117 (2009) 450.

[4] B. Gil, J. Janas, E. Włoch, Z. Olejniczak, J. Datka, B. Sulikowski, Catal. Today 137 (2008) 174.

[5] S. Satokawa, Chem. Lett. 29 (2000) 294.

[6] J.P. Breen, R. Burch, Top. Catal. 39 (2006) 53.

[7] S.T. Korhonen, A.M. Beale, M.A. Newton, B.M. Weckhuysen, J. Phys. Chem. C 115 (2011) 885.

[8] M.M. Azis, H. Härelind, D. Creaser, Catal. Sci. Technol. 5 (2015) 296.

[9] K. Shimizu, M. Tsuzuki, K. Kato, S. Yokota, K. Okumura, A. Satsuma. J. Phys. Chem. C 111 (2007) 950.

[10] K. Shimizu, K. Sugino, K. Kato, S. Yokota, K. Okumura, A. Satsuma, J. Phys. Chem. C, 111 (2007) 6481.

[11] K. Shimizu, K. Sawabe, A. Satsuma, Catal.Sci.Technol.1 (2011) 331.

[12] Y. B. Yu, H. He, X. L. Zhang, H. Deng, Catal.Sci.Technol. 4 (2014) 1239.

ACCEPTED MANUSCRIPT

[13] R. Burch, J.P. Breen, C.J. Hill, B. Krutzsch, B. Konrad, E. Jobson, L. Cider, K. Eranen, F. Klingstedt, L-E. Lindfors, Top. Catal. 30-31 (2004) 19.

[14] P. Sazama, L. Čapek, H. Drobná, Z. Sobalık, J. Dědeček, K. Arve, B. Wichterlová, J. Catal. 232 (2005) 302.

[15] K. Eranen, F. Klingstedt, K. Arve, L.E. Lindfors, D.Y. Murzin, J. Catal. 227 (2004) 328.

[16] J. Shibata, Y. Takada, A. Shichi, S. Satokawa, A. Satsuma, T. Hattori, Appl. Catal., B 54 (2004) 137.

[17] A. Sultana, M. Haneda, T. Fujitani, H. Hamada, Catal. Lett. 114 (2007) 96.

[18] Y. Yan, Y. Yu, H. He, J. Zhao, J. Catal. 293 (2012) 13.

[19] P. Kyriienko, N. Popovych, S. Soloviev, S. Orlyk, S. Dzwigaj, Appl. Catal., B. 140-141 (2013) 691.

[20] N. Popovych, P. Kyriienko, S. Soloviev, S. Orlyk, S. Dzwigaj, Microporous Mesoporous Mater. 203 (2015) 163.

[21] S. Dzwigaj, M.J. Peltre, P. Massiani, A. Davidson, M. Che, T. Sen, S. Sivasanker, Chem. Commun. 1 (1998) 87.

[22] S. Dzwigaj, M. Matsuoka, R. Franck, M. Anpo, M. Che, J. Phys. Chem. B 102 (1998) 6309.

[23] S. Dzwigaj, Curr. Opin. Solid State Mater. Sci. 7 (2003) 461.

[24] S. Dzwigaj, E. Ivanova, R. Kefirov, K. Hadjiivanov, F. Averseng, J.M. Krafft, M.Che, Catal. Today 142 (2009) 185.

[25] S. Dzwigaj, Y. Millot, J.-M. Krafft, N. Popovych, P. Kyriienko, J. Phys. Chem. C 117 (2013) 12552.

[26] S. Dzwigaj, N. Popovych, P. Kyriienko, J.-M. Krafft, S. Soloviev, Microporous Mesoporous Mater. 182 (2013) 16.

[27] M.A. Camblor, A. Corma, J. Pérez-Pariente, Zeolites 13 (1993) 82.

[28] J.S. Reddy, A. Sayari, Stud. Surf. Sci. Catal. 94 (1995) 309.

ACCEPTED MANUSCRIPT

[29] S. Dzwigaj, P. Massiani, A. Davidson, M. Che, J. Mol. Catal. A 155 (2000) 169.

[30] E. Bourgeat Lami, F. Fajula, D. Anglerot, T. Des Courieres, Microporous Mater. 1 (1993) 237.

[31] K. Hadjiivanov, A. Penkova, R. Kefirov, J. Janas, A. Plesniar, S. Dzwigaj, M. Che, Microporous Mesoporous Mater. 131 (2010) 1.

[32] K. Chakarova, K. Hadjiivanov, J. Phys. Chem. C 115 (2011) 4806.

[33] K. Hadjiivanov, G. Vayssilov, Adv. Catal. 47 (2002) 307.

[34] K. Hadjiivanov, A. Penkova, M. Centeno, Catal. Commun. 8 (2007) 1715.

[35] B.H. Chiche, F. Fajula, E. Garrone, J. Catal. 146 (1994) 460.

[36] B. Gil, S.I. Zones, S-J. Hwang, M. Bejblova, J. Čejka. J. Phys. Chem. C 112 (2008) 2997.

[37] K.A. Bethke, H.H. Kung, J. Catal. 93 (1997) 172.

[38] N. Bogdanchikova, F.C. Meunier, M. Avalos-Borja, J.P. Breen, A. Pestryakov, Appl. Catal., B 36 (2002) 287.

[39] A. Satsuma, J. Shibata, A. Wada, Y. Shinozaki, T. Hattori, Stud. Surf. Sci. Catal. 145 (2003) 235.

[40] J. Shibata, Y. Takada, A. Shichi, S. Satokawa, A. Satsuma, T. Hattori, J. Catal. 222 (2004) 368.

[41] N. D. Hutson, B. A. Reisner, R. T. Yang, B. H. Toby, Chem. Mater. 12 (2000) 3020.

[42] W. Ju, M. Matsuoka, K. Iino, H. Yamashita, M. Anpo, J. Phys. Chem. B 108 (2004) 2128.

[43] H. He, Y. Li, X. Zhang, Y. Yu, C. Zhang, Appl. Catal. A 375 (2010) 258.

[44] X. Zhang, H. He, H. Gao, Y. Yu, Spectrochim. Acta, Part A 71 (2008) 1446.

[45] Y. Yu, Y. Li, X. Zhang, H. Deng, H. He, Y. Li, Environ. Sci. Technol. 49 (2015) 481.

[46] P. Sazama, B. Wichterlova, Chem. Commun. 38 (2005) 4810.

[47] C. Thomas, Appl. Catal., B 162 (2015) 454-462.

[48] H. Kannisto, H.H. Ingelsten, M. Skoglundh, Top. Catal. 52 (2009) 1817.

ACCEPTED MANUSCRIPT

[49] N. A. Sadokhina, A. V. Bukhtiyarov, A. I. Mytareva, R. I. Kvon, V. I. Bukhtiyarov, A. Yu. Stakheev, Top Catal. 56 (2013) 187.

[50] K. Shimizu, J. Shibata, A. Satsuma, J. Catal. 239 (2006) 402.

[51] P. Hirunsit, K. Shimizu, R. Fukuda, S. Namuangruk, Y. Morikawa, M. Ehara, J. Phys. Chem. C 118 (2014) 7996.

ACCEPTED MANUSCRIPT

ACCEPTED MANUSCRIPT

Figure captions

Fig. 1 XRD patterns recorded at room temperature.

Fig. 2 FT-IR spectra recorded at room temperature of the samples calcined at 773 K (3 h) in flowing air and then outgassed at 573 K (10^{-3} Pa, 2 h).

Fig. 3 FT-IR difference spectra (OH stretching region) of samples after adsorption of CO at 100 K: equilibrium CO pressure of 100 Pa (a) and development of the spectra during evacuation for about 0.5 h at 100 K up to 10^{-3} Pa (b–f).

Fig. 4 FT-IR difference spectra (carbonyl stretching region) of CO adsorbed at 100 K on samples: equilibrium CO pressure of 100 Pa (a) and development of the spectra during evacuation for about 0.5 h at 100 K up to 10^{-3} Pa (b–f). The spectra are background corrected.

Fig. 5 FT-IR difference spectra recorded at room temperature of the samples after calcination at 773 K for 1 h in O_2 ($2 \cdot 10^4$ Pa), outgassing at 673 K (10^{-3} Pa) for 1 h, adsorption of pyridine at 423 K and desorption of pyridine at 423 K (a), 573 K (b), 673 K (c).

Fig. 6 FT-IR difference spectra recorded at room temperature of the samples after reduction at 773 K for 1 h in H_2 flow, outgassing at 673 K (10^{-3} Pa) for 1 h, adsorption of pyridine and desorption 423 K.

Fig. 7 DR UV-Vis spectra of the samples after pre-treatment in the conditions of the SCR-process.

Fig. 8 Temperature dependences of NO conversion in the SCR with ethanol (*– in the presence of H_2 in the reaction mixture) on: (A) 1 – AlSiBEA(100), 2 – $Ag_{0.5}$AlSiBEA(100), 3 – $Ag_{1.5}$AlSiBEA(100), 4 – $Ag_{3.0}$AlSiBEA(100), (B) 5 – AlSiBEA(200), 6 – $Ag_{0.5}$AlSiBEA(200), 7 – $Ag_{1.5}$AlSiBEA(200), 8 – $Ag_{3.0}$AlSiBEA(200).

Fig. 9 Temperature dependences of ethanol conversion in the SCR of NO to CO_2 (1-■-□-), CO (2-●-○-) and C_2H_4 (3-▲-Δ-) (*– in the presence of H_2 in the reaction mixture).

Fig. 10 Dependence of increase in NO conversion in the SCR process on the Si/Al ratio of AgBEA catalysts after H_2 addition.

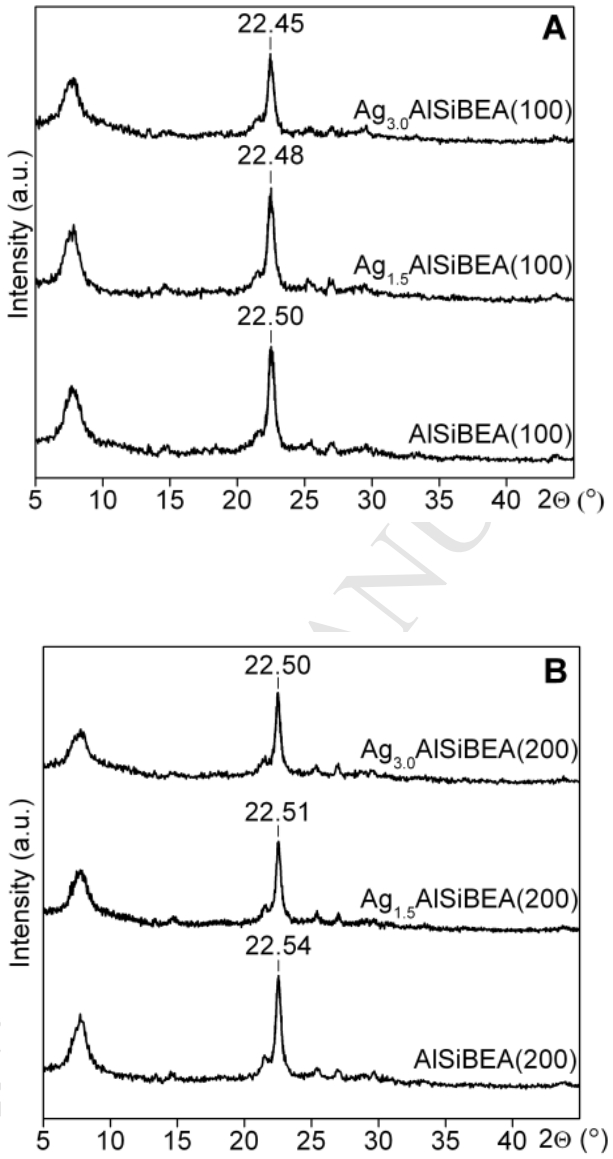
A
22.45
Ag3.0AlSiBEA(100)
22.48
Ag1.5AlSiBEA(100)
22.50
AlSiBEA(100)
Intensity (a.u.)
5 10 15 20 25 30 35 40 2Θ (°)
B
22.50
Ag3.0AlSiBEA(200)
22.51
Ag1.5AlSiBEA(200)
22.54
AlSiBEA(200)
Intensity (a.u.)
5 10 15 20 25 30 35 40 2Θ (°)

Fig. 1.

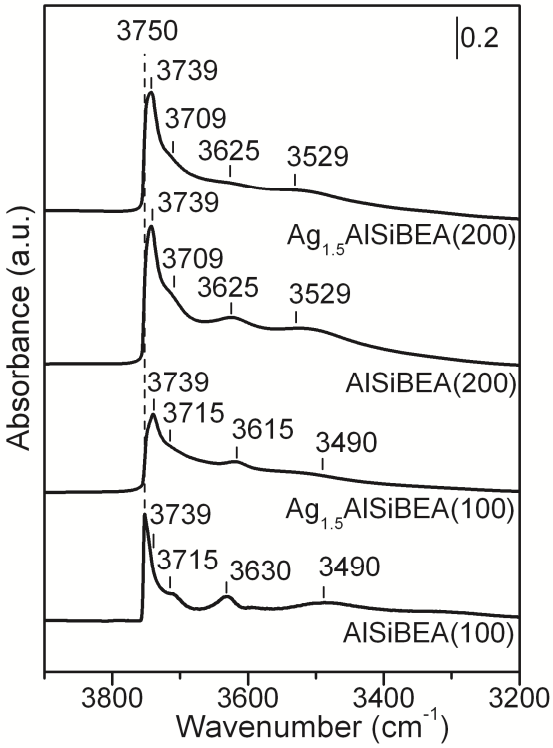

Fig. 2.

ACCEPTED MANUSCRIPT

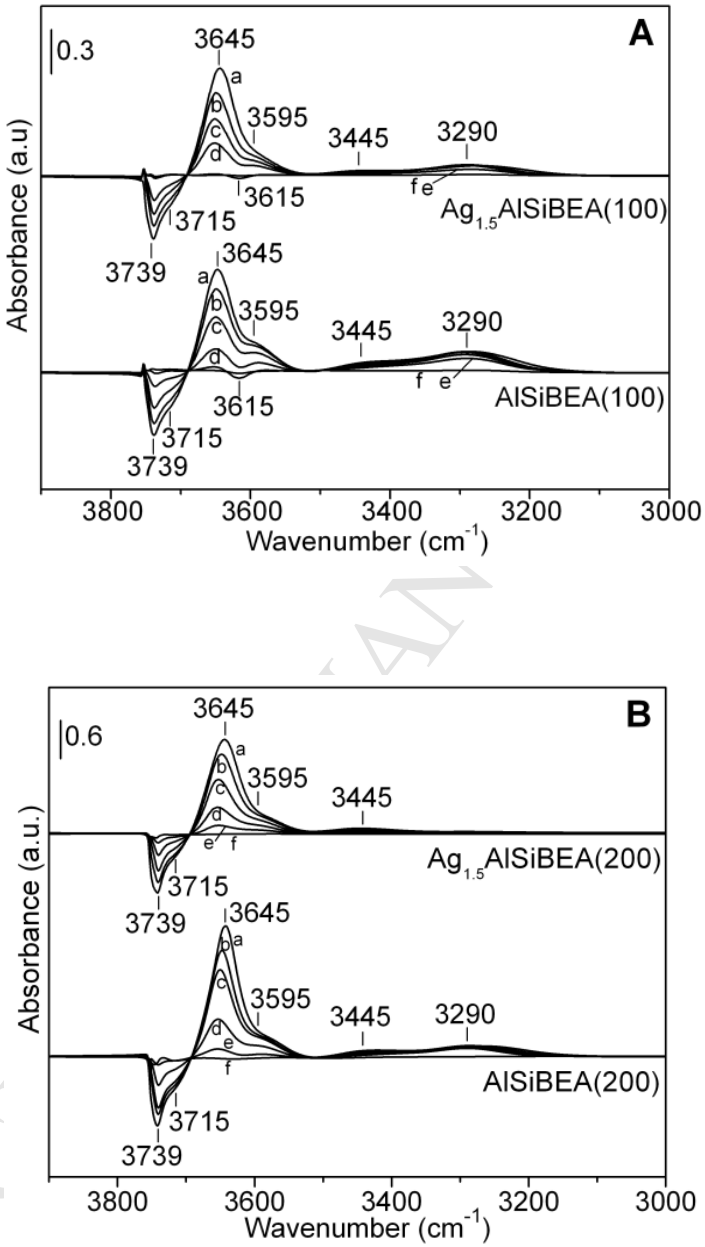
A
0.3
3645
a
b
c
d
3595
3445
3290
f e
3615
3715
3739
Ag1.5AlSiBEA(100)
3645
a
b
c
d
3595
3445
3290
f e
3615
3715
3739
AlSiBEA(100)
Absorbance (a.u)
3800
3600
3400
3200
3000
Wavenumber (cm-1)
B
0.6
3645
a
b
c
d
e f
3595
3445
3715
3739
Ag1.5AlSiBEA(200)
3645
a
b
c
d
e
f
3595
3445
3290
3715
3739
AlSiBEA(200)
Absorbance (a.u.)
3800
3600
3400
3200
3000
Wavenumber (cm-1)

Fig. 3.

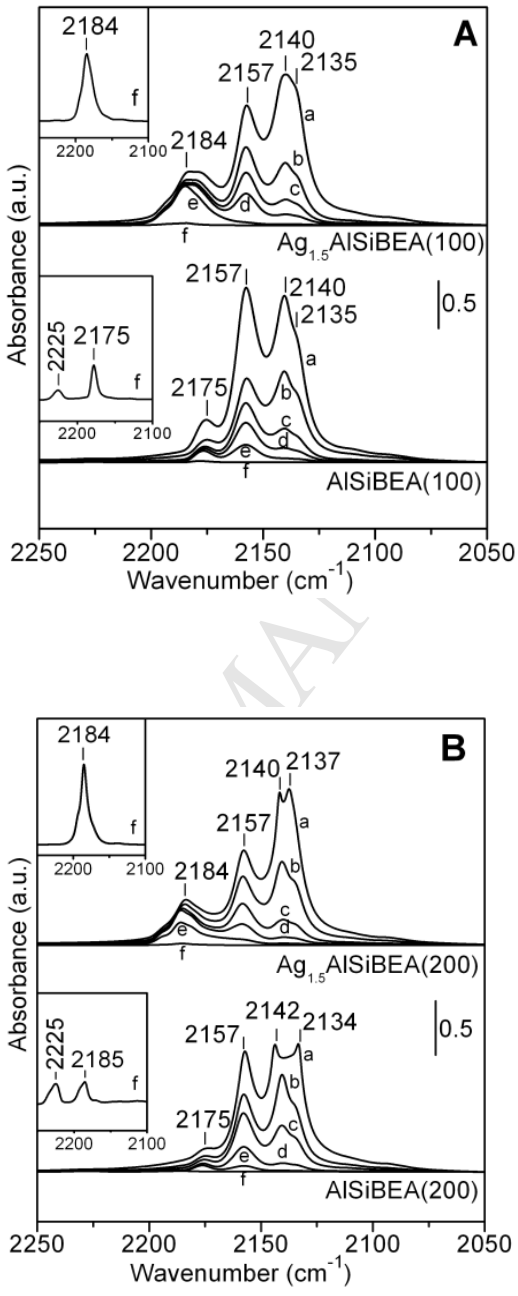
A
2184
2140
2157
2135
a
b
c
d
e
f
2200
2100
Ag1.5AlSiBEA(100)
2225
2175
0.5
AlSiBEA(100)
Absorbance (a.u.)
2250
2200
2150
2100
2050
Wavenumber (cm-1)
B
2137
2142
2134
2185
Ag1.5AlSiBEA(200)
AlSiBEA(200)

Fig. 4.

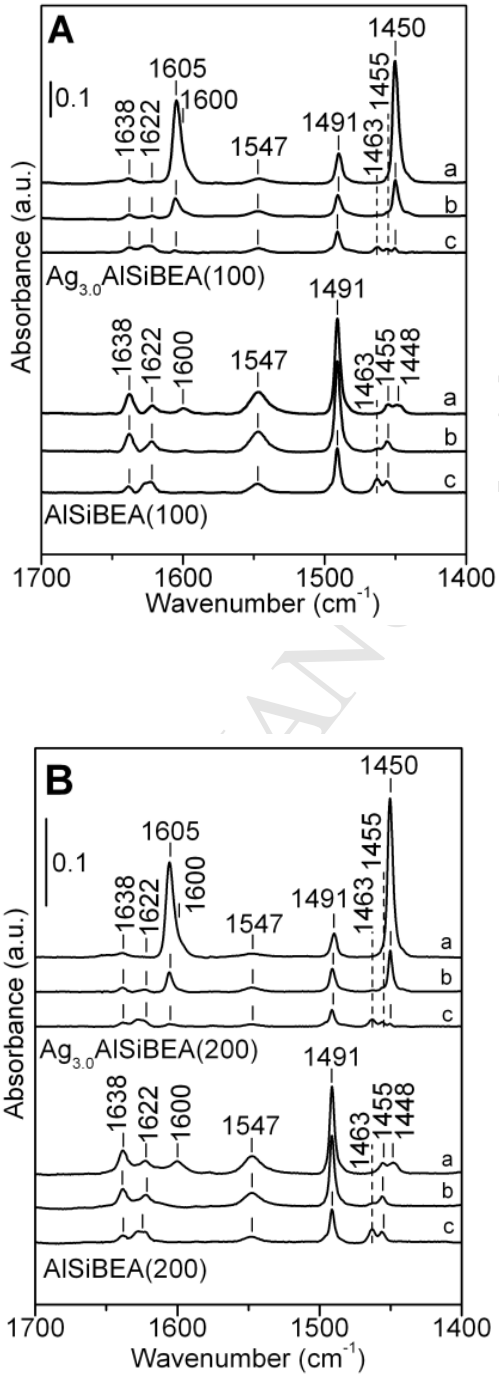
A
0.1
1638
1622
1605
1600
1547
1491
1463
1455
1450
a
b
c
Ag3.0AlSiBEA(100)
1638
1622
1600
1547
1491
1463
1455
1448
a
b
c
AlSiBEA(100)
Absorbance (a.u.)
1700
1600
1500
1400
Wavenumber (cm-1)
B
0.1
1638
1622
1605
1600
1547
1491
1463
1455
1450
a
b
c
Ag3.0AlSiBEA(200)
1638
1622
1600
1547
1491
1463
1455
1448
a
b
c
AlSiBEA(200)
Absorbance (a.u.)
1700
1600
1500
1400
Wavenumber (cm-1)

Fig. 5.

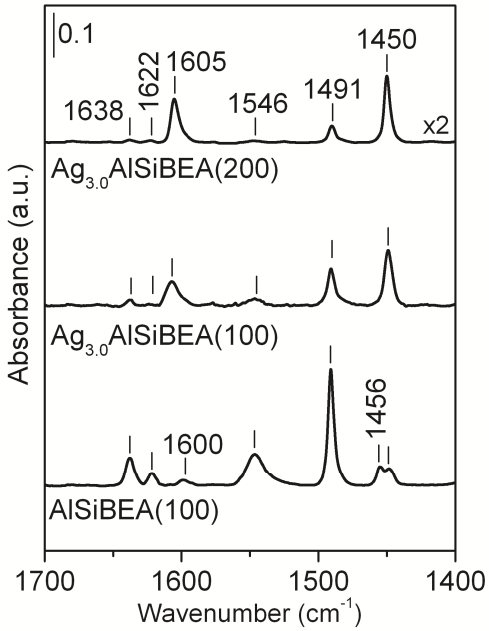
0.1
1450
1605
1622
1638
1546
1491
x2
Ag3.0AlSiBEA(200)
Absorbance (a.u.)
Ag3.0AlSiBEA(100)
1456
1600
AlSiBEA(100)
1700
1600
1500
1400
Wavenumber (cm-1)

Fig. 6.

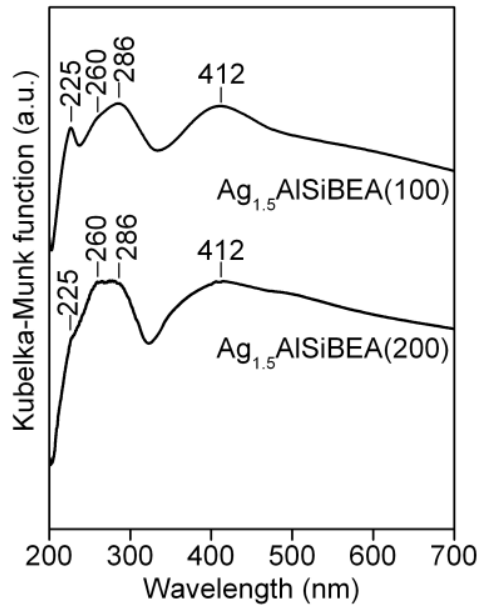
225
260
286
412
Ag1.5AlSiBEA(100)
Kubelka-Munk function (a.u.)
225
260
286
412
Ag1.5AlSiBEA(200)
200
300
400
500
600
700
Wavelength (nm)

Fig. 7.

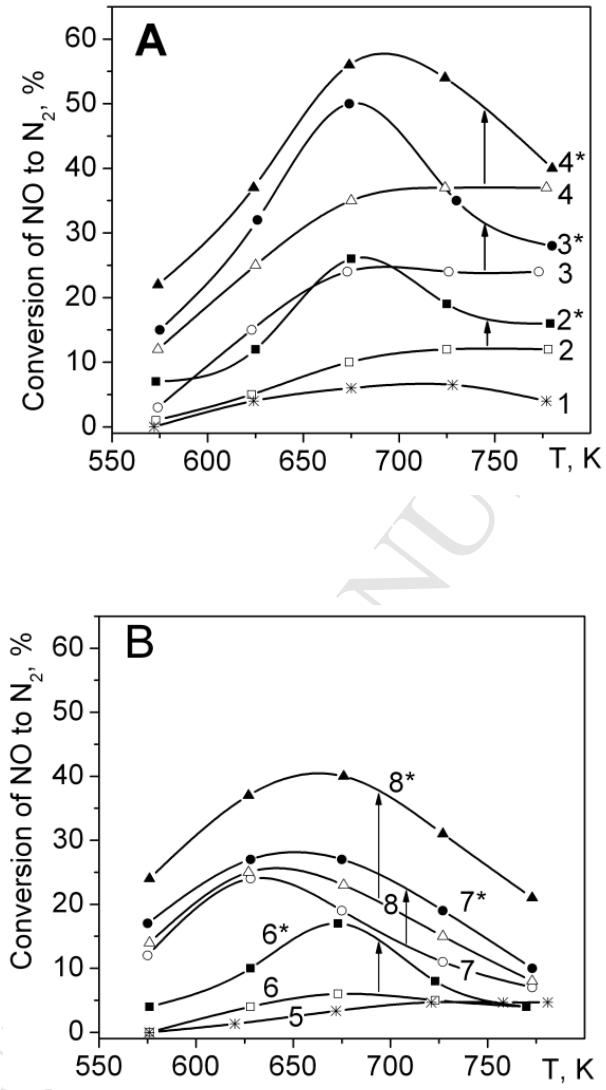
A
Conversion of NO to N2, %
T, K
4*
4
3*
3
2*
2
1
B
Conversion of NO to N2, %
T, K
8*
7*
8
6*
7
6
5

Fig. 8.

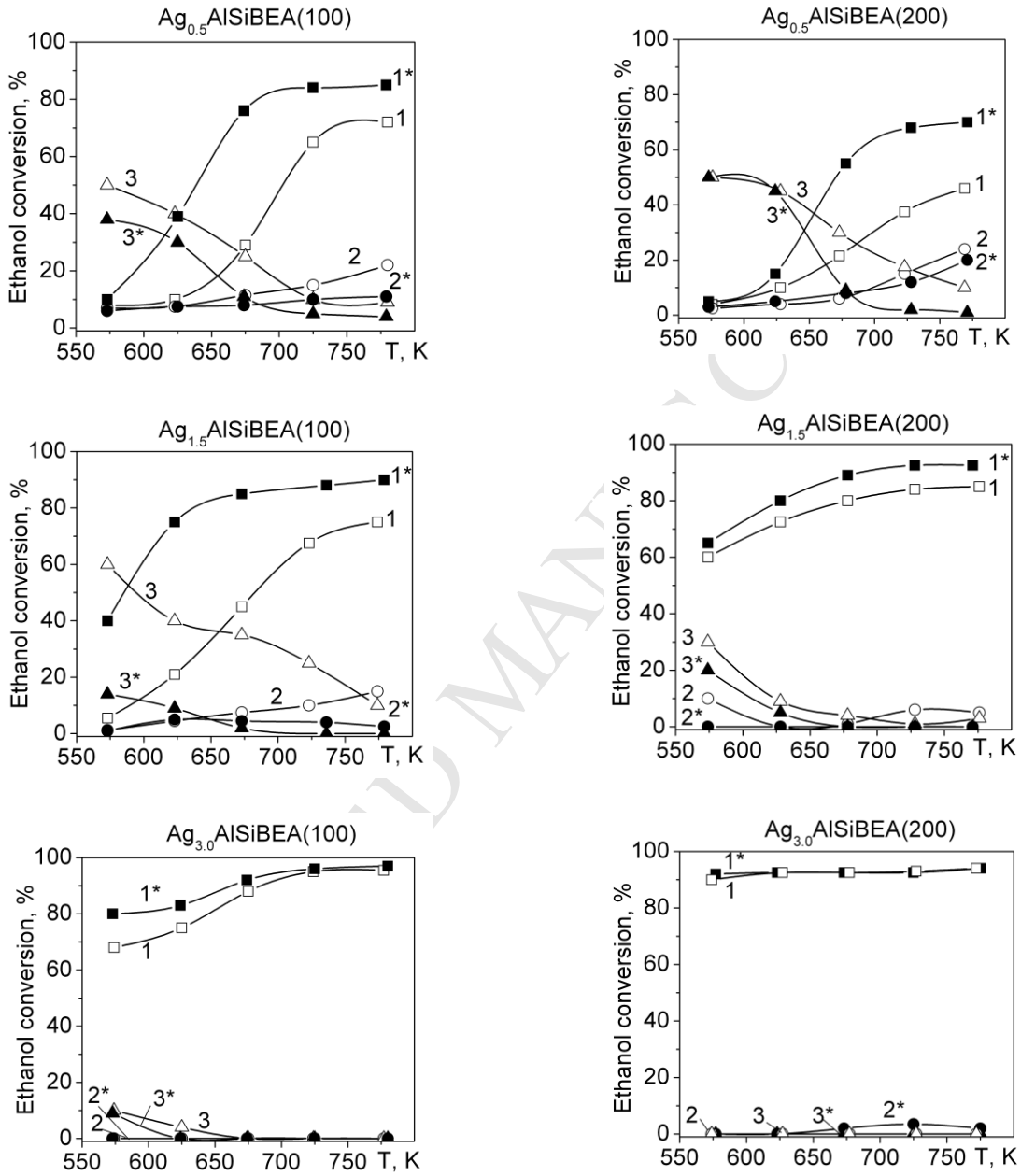
Ag0.5AlSiBEA(100)
Ag0.5AlSiBEA(200)
Ag1.5AlSiBEA(100)
Ag1.5AlSiBEA(200)
Ag3.0AlSiBEA(100)
Ag3.0AlSiBEA(200)
Ethanol conversion, %
T, K
1*
1
2
2*
3
3*

Fig. 9.

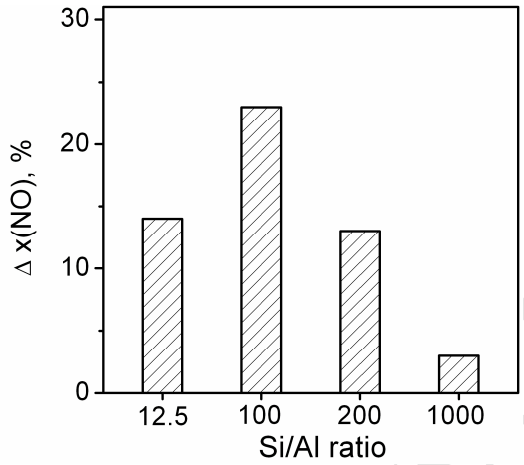

Fig. 10.

ACCEPTED MANUSCRIPT

ACCEPTED MANUSCRIPT

- Two-step postsynthesis allowed obtaining catalysts with Si/Al ratio of 200 and 100.

- H_2-promoting effect on the SCR of NO depended on dealumination degree of zeolite.

- Greater H_2-effect observed on catalysts with higher amount of acidic sites.

ACCEPTED MANUSCRIPT